MECHANICAL BEHAVIOR UNDER COMPRESSION OF LOW-DENSITY METAL-MATRIX COMPOSITES FOR IMPACT ENERGY ABSORBERS

Alexandre Fonseca Jorge
Antonio Celso Fonseca de Arruda
Maria Helena Robert
Faculty of Mechanical Engineering, University of Campinas. Campinas /SP/ Brazil

Abstract. *A new composite material, produced by thixoinfiltration process, based on aluminum alloy AA7075 as matrix reinforced with porous, light ceramic particles, is presented. The mechanical behavior of the new material under compressive load is analysed, and related to their density and internal architecture (volumetric fraction and dispersion of reinforcement, metallic walls thickness, microstructure of metallic walls and metal/reinforcement interface). Two different types of reinforcement are used: foamed spheroidal ceramic particles and vermicular particles. The mechanisms of deformation and rupture are analysed in the different types of composites produced.*

Keywords: *composites, thixoinfiltration.*

1. INTRODUCTION

In the last decades, there has been an increasing demand for new engineering materials, which can gather an interesting set of properties that otherwise would be difficult or even impossible to be obtained with conventional materials.

Two recently demanding areas of interest are lightweight materials and energy-absorbing materials, sought especially by the transportation industry which is constantly aiming for improvements in fuel efficiency and safety.

In that context, low-density composites, combining a metallic matrix with porous ceramic reinforcement, in a cellular-like arrangement, can represent a new interesting class of lightweight materials, combining properties of conventional composites and cellular materials. Those materials can be considered to be related to the development of cellular materials, particularly syntactic foams.

This work investigates the possibility of the production by thixoinfiltration of composites with a metallic-alloy matrix and reinforcements constituted by porous ceramic particles. The use of semi-solid metallurgy implies in lower temperatures and easier controllability of the production processing, if compared to liquid metal processes (Kirkwood, 2010). The process can be also used for the production of cellular metallic materials (Silva, 2009).

Besides their production, their internal architecture, microstructure, and mechanical properties are also investigated, particularly their compression behavior, which can allow an initial evaluation of their suitability as mechanical energy absorption materials.

Also, the deformation mechanisms are analysed and correlated to the mechanical behavior observed.

2. MATERIALS AND METHODS

2.1. Production of samples

For the production of the materials, the alloy used was AA7075, with main composition (in weight %): Al, 5.1%Zn, 2.2%Mg and 1.5%Cu. It is a commercial alloy with high percentage of alloying elements, and thermally treatable (Hatch, 1993). The alloy presents a wide solidification range, between T(solidus) of 480ºC and T(liquidus) of 640ºC, approximately. That characteristic makes the alloy suitable for semi-solid processing, providing an easier control of the process parameters.

As reinforcement materials, particles of vermiculite and expanded clay were used. Those materials consist of low-density ceramic porous particles, both composed mainly by silica, alumina, and other oxides. They are stable at high temperatures, and chemically inert in contact with metal. Both materials were classified in two different granulometries for this work: Fine: between 1.60mm and 3.15mm; and Coarse, between 3.15 mm and 5.00 mm.

Figure 1 shows the aspect of vermiculite particles and their internal structure. Vermiculite is a mineral, found in nature in non-expanded form. Under high temperatures it expands uniaxially, resulting in soft particles with vermicular geometry and lamellar structure. As consequence, they have an extremely low density between 0.08 and 0.14 g/cm^3.

Figure 2 shows the aspect of expanded clay particles and their internal structure. They are rounded, almost spheroidal particles, with high hardness, and fragile rupture. They are very porous internally, with a low density of approximately 0.85g/cm^3.

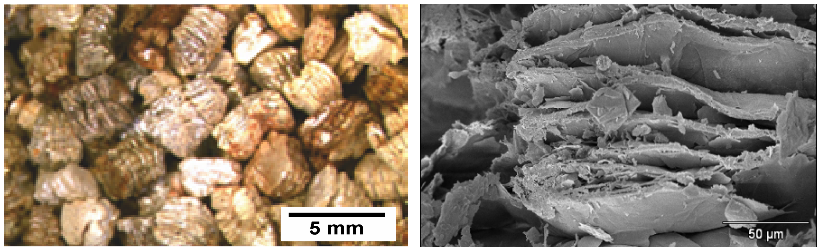

Figure 1: Aspect of expanded vermiculite particles, and SEM microscopy image showing their porous lamellar structure.

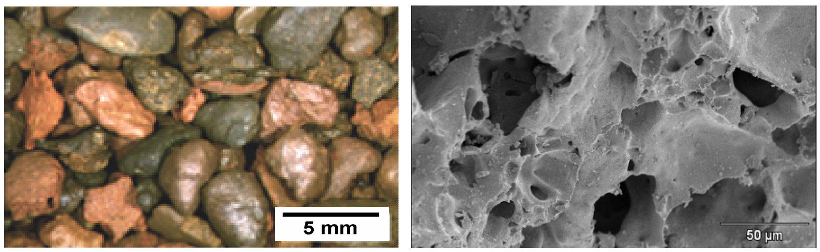

Figure 2: Aspect of expanded clay particles, and SEM microscopy image showing their interior porous structure.

For the production of the composite materials, a preform of ceramic particles is placed inside a metallic mold, and covered with a layer of AA7075 alloy, in a suitable proportion between metal and reinforcement. The full assembly is heated until the alloy reaches temperatures in the higher end of the semi-solid range, suitable for the formation of the thixotropic paste. Then, the alloy is infiltrated into the preform (in the voids between particles), through the application of pressure. Fig. 3 shows a simplified scheme of the processing (Jorge, 2010). Four different types of composites, combining the two different particles, expanded vermiculite and expanded clay, and two different granulometries, fine and coarse, were produced.

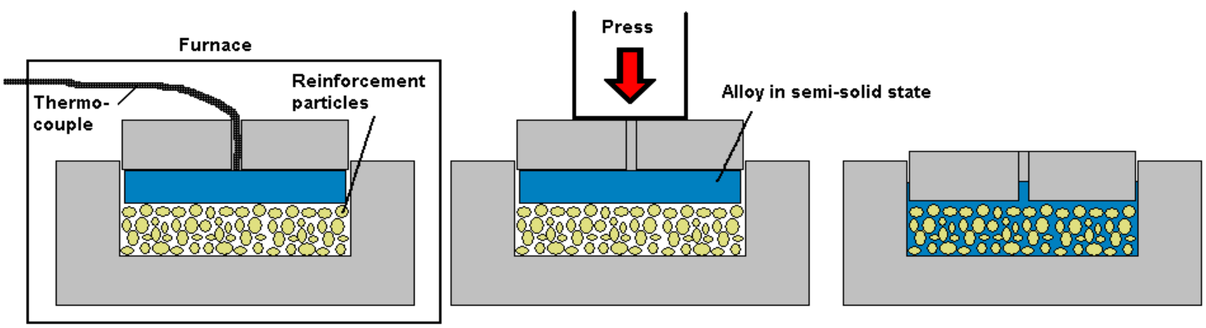

Figure 3: Simplified sequence showing the thixoinfiltration process employed: controlled heating, infiltrartion through the application of pressure, and final product before disassembling the mold.

2.2. Description of tests for characterization of the products

After production, the density of the samples of the composites produced was determined by using a Helium gas pycnometer. Also they were submitted to macro and micrography analysis, in order to study their internal architecture, and microstructure of the metallic matrix.

Some samples of the materials underwent compression tests, in a servo-mechanical traction/compression machine model Instron 5500R, equipped with a load-cell of 25000 kgf. The tests consisted of semi-static compression between parallel plates, with free sides, and a strain rate of approximately $10s^{-1}$. Using the data acquired during the testing, it was possible to obtain the stress-strain curves of the compression of the samples. The compression tests were conducted in two different ways: first a normal semi-static test, and after that, interrupted semi-static compression tests. The interrupted tests were performed to provide partially compressed samples, to make it possible to study the internal deformation mechanisms.

3. RESULTS AND DISCUSSION

3.1 Obtained products

Figures 4 and 5 show images of the external aspect of typical composites produced. It is possible to observe a good distribution of the reinforcement particles through the metallic matrix in all cases. Apparently, in the external surfaces of the materials produced, the reinforcement particles are more hidden by the metallic layer, showing a tendency to form a metallic skin. So, transversal sections of the samples were taken, as a better representation of the internal architecture in all cases.

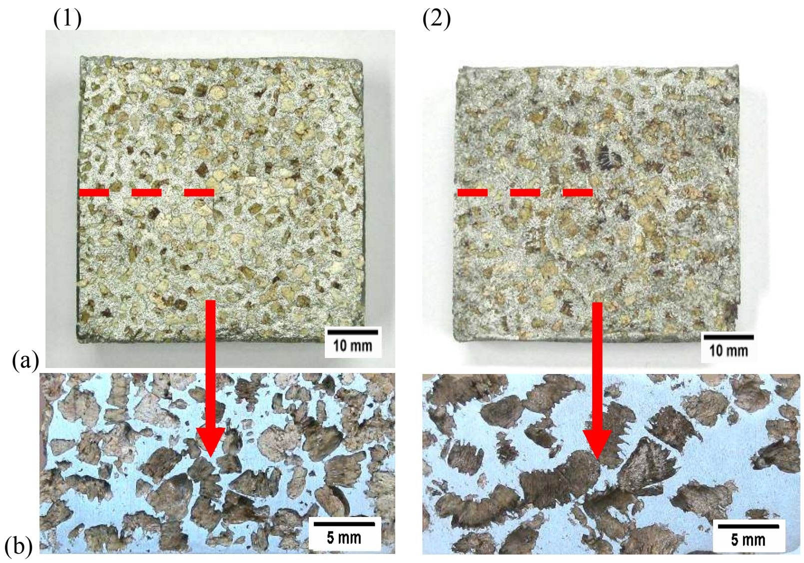

Figure 4. (a) External aspect of typical AA7075 composites produced with vermiculite in two different granulometries: (1) fine and (2) coarse; (b) Transversal sections as indicated.

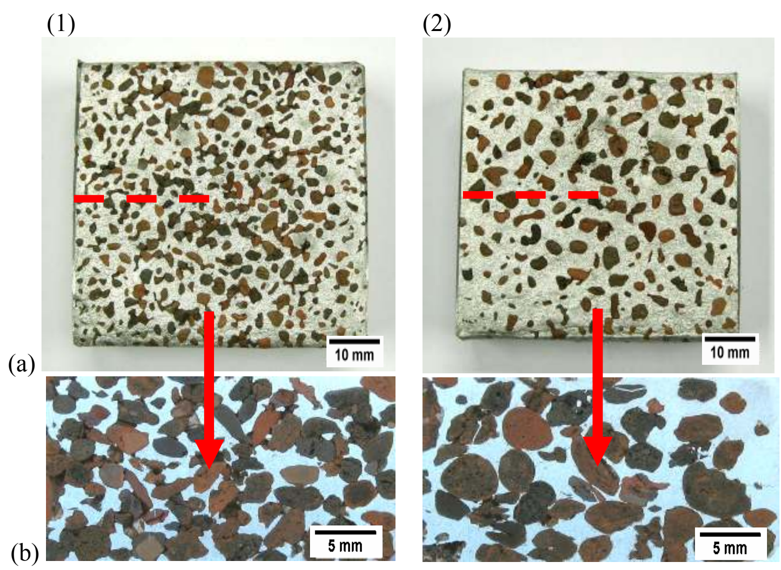

Figure 5. (a) External aspect of typical AA7075 composites produced with expanded clay in two different granulometries: (1) fine and (2) coarse; (b) Transversal sections as indicated.

In general terms, even though the reinforcement particles had an aleatory geometry, orientation and localization, the distribution can be considered reasonably uniform in macroscopical scale. That kind of distribution of the reinforcement particles is very similar to the distribution of pores in a cellular material. Additionally, for the composites with vermiculite particles, it is observed that the metallic alloy can be infiltrated into the open porosities of most of the particles, resulting in a good mechanical coupling between matrix and reinforcement.

Figure 6 (a-d) shows optical microscopy images of samples of the composites produced with vermiculite and expanded clay. It is possible to observe, in all cases, that the microstructure of metallic walls is mainly composed by fine equiaxial dendrites. It is also possible to observe the presence of precipited components near the borders of the dendrites, and a layer of eutectic component between them, or sometimes trapped into them.

Even though the alloy was infiltrated in its semi-solid state, the resulting microstructure was not predominantely globular, because in infiltration processes through narrow voids, the liquid fraction of the slurry has a tendency to infiltrate faster and more easily than its solid fraction. As a result, the metallic walls were mainly formed by the liquid fraction, which after solidification became dendritic.

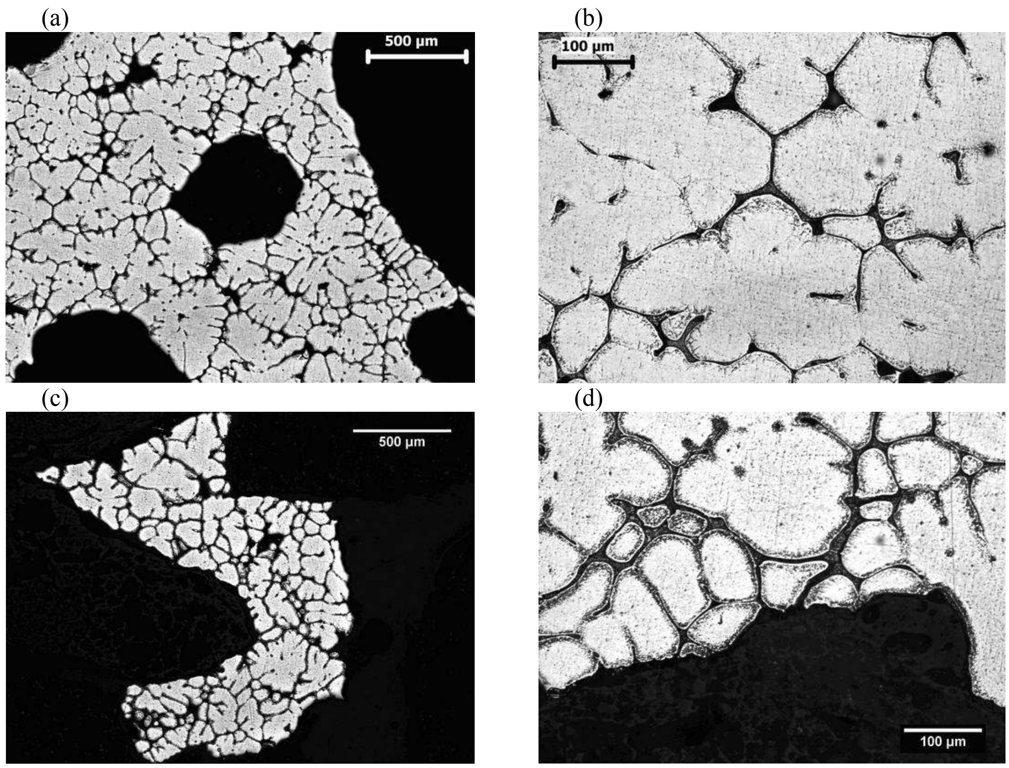

Figure 6: Optical microscopy images, in two magnification levels, of the metallic walls from the produced materials: (a,b) composites with vermiculite; (c,d) composites with expanded clay. Samples etched with modified Keller’s reagent.

3.2 Density of the obtained products

Figure 7 shows the average values of density of the produced composites, obtained by pycnometry analysis. The composites with vermiculite particles show lower densities if compared with the composites with expanded clay. That difference in density is attributed mainly by the lower density of the expanded vermiculite particles (between 0.08 and 0.14 $g/cm^{3)}$ in comparison with the expanded clay particles (circa $0.85 g/cm^3$). Despite of that, the granulometry of the particles has little effect on the density results, indicating a similar ratio between matrix and reinforcement with the different granulometries.

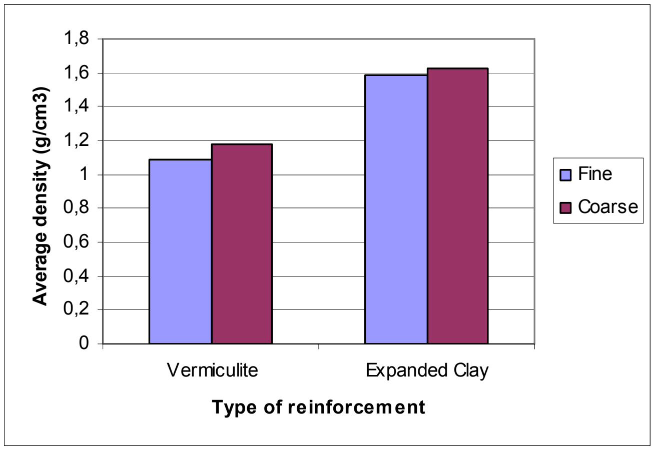

Figure 7: Average density of the produced composites, according to the different types of reinforcements and particle dimensions employed.

3.3 Matrix-reinforcement volume ratio

The produced composites also underwent macro image analysis, and the images of their internal sections were processed for the calculation of the estimated volume ratio of metallic matrix and reinforcement for each material. Figure 8 shows the results obtained, related to the reinforcement. Despite their lower density, the vermiculite composites had also a lower volume fraction of reinforcement. The probable factors that contributed for this result were the lower density of vermiculite particles if compared to expanded clay, and the geometry of those particles, with the presence of open porosities that were mostly filled with the metallic alloy during the infiltration process (which contributed to a higher fraction of metallic matrix), in contrast with the expanded clay particles which had almost no open porosities.

Another observed characteristic, for both types of reinforcement, is the higher reinforcement volume ratio that occurred with the fine granulometry. That probably is a consequence of the more difficult infiltration of the alloy between lower-granulometry particles, since the interstitial space between them is proportionally smaller. Also, there can be more accommodation between particles in that case, which also contributes for smaller interstitial spaces.

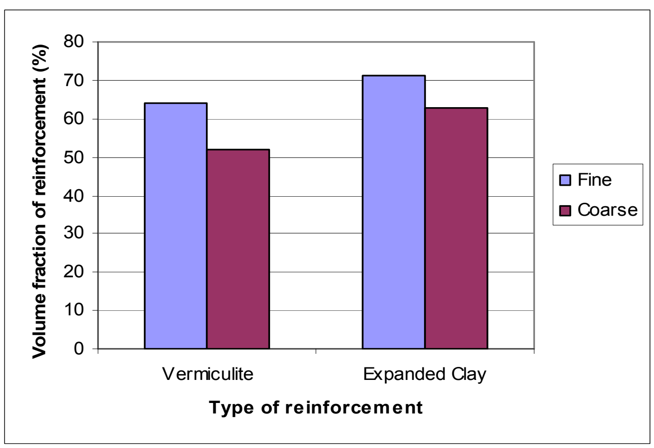

Figure 8: Volume fraction of reinforcements in the composites, according to the different types of reinforcements and granulometries employed, obtained by macro analysis.

3.4 Semi-static compression tests

Complete compression tests were performed with each type of composite, in order to analyse their overall behavior aind to determine critical points in stress/strain curve. Further tests were performed and interrupted at those points. The basic features of the obtained stress-strain curves were similar to the typical ones from cellular metals (Motz, 2002) (Ashby, 2000), with an initial mainly elastic phase, followed by a plastic phase in “plateau” (large strain interval with almost constant stress), and a densification stage at the end. The only difference was a high stress peak in the region between the elastic and plastic regions. The stress level in which the transition between these two stages of the curve occur is called compression stress. After that, there is a decline in stress before the stabilization of the plastic plateau. So, the stages for interruption of the tests were set, according to Fig. 9, to approximately:

1) Immediately after compression stress
2) At the beginning of the plastic plateau
3) In the middle of the plastic plateau
4) At the beginning of densification (or at 60% strain if the densification was not evident until then)

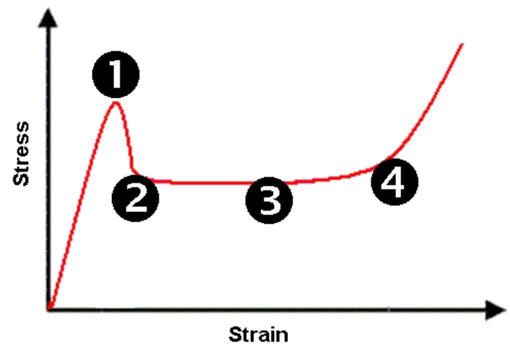

Figure 9: Scheme illustrating the four different stages of interrupted compression tests.

Figures 10 and 11 show the stress-strain curves obtained from the interrupted compression tests, respectively for the composites with vermiculite and expanded clay particles. It can be observed that, as said previously, the stress-strain curves all present the same basic shape. There is a initial high slope region, almost linear, corresponding mainly to the elastic stage. The stresses raise up to a peak value, which is considered the compression stress for these materials, being in the range near 20 MPa for vermiculite composites, and near 40 MPa for expanded clay composites. After that, there is an important fall in the stress levels, by >10MPa for vermiculite composites, and >20MPa for expanded clay composites, approximately. That extreme difference between the peak and plateau suggests the occurrence of a fragile rupture of the metallic walls. However, the slope of the descending curve is not extremely high, which is probably caused by the presence of the reinforcements, acting as a damping element and not allowing a catastrophic failure of the cellular structure.

The plateau stresses for all materials show some fluctuations and some dispersion among tested samples, but they were sustained for a large strain range. It is possible to observe that the granulometry has the major influence in plateau levels, for both types of composite particles, with the coarse granulometries leading to higher plateau stresses, if compared to the respective fine granulometries. The densification starts to occur at around 45-55% strain for vermiculite, and with higher strains for expanded clay composites.

Comparing the results of vermiculite and expanded clay composites, it can be observed that the expanded clay composites present values for the compression stress that were approximately 100% higher than the compression stress observed with vermiculite composites. That is considered to be caused by the high stiffness of the expanded clay particles, which act as a structural component, differently than the vermiculite particles that are soft and compressible. The plateau stresses are at similar levels for the two types of composites, although with high dispersion of results and fluctuations, especially for the coarse granulometries. Finally, the densification occurred earlier with the vermiculite composites than with the expanded clay composites. That probably happened because the vermiculite particles act as a cohesion agent during the compression, resulting in a less fragmented sample, which has a proper densification under higher strains. On the other hand, the expanded clay composite looses many fragments during the final stages of deformation, reducing its densification.

For impact applications, it can be considered, with the proper scale factors related to the higher strain rate, that the compression behavior would be similar to the semi-static case, even though rougher curves and higher stress values are expected (Motz, 2002).

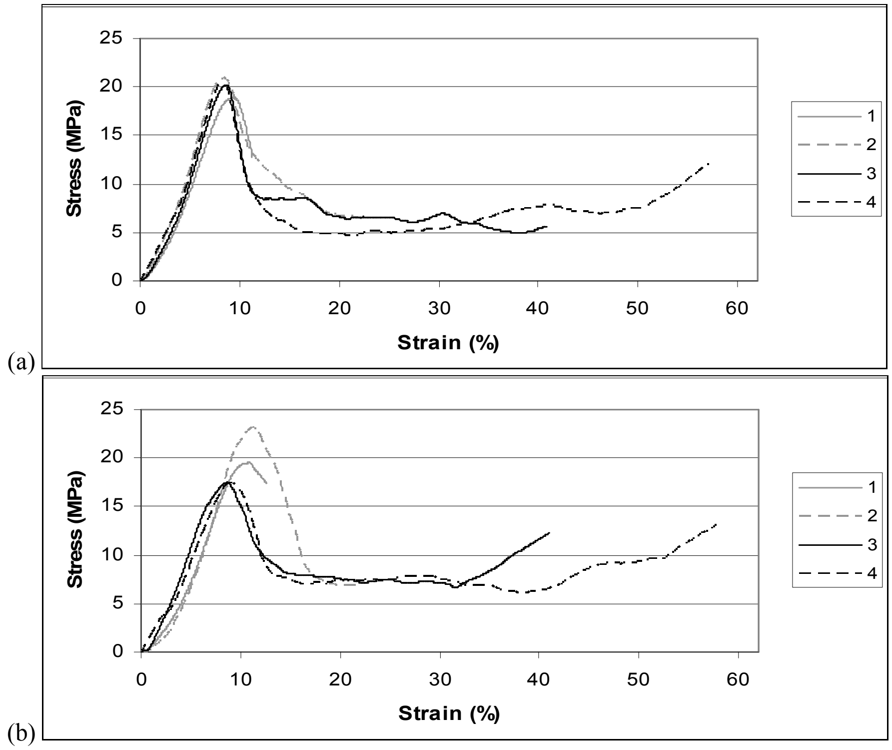

Figure 10. Stress-strain curves obtained from the four-stage interrupted compression tests of the composites with vermiculite particles: (a) fine granulometry; (b) coarse granulometry.

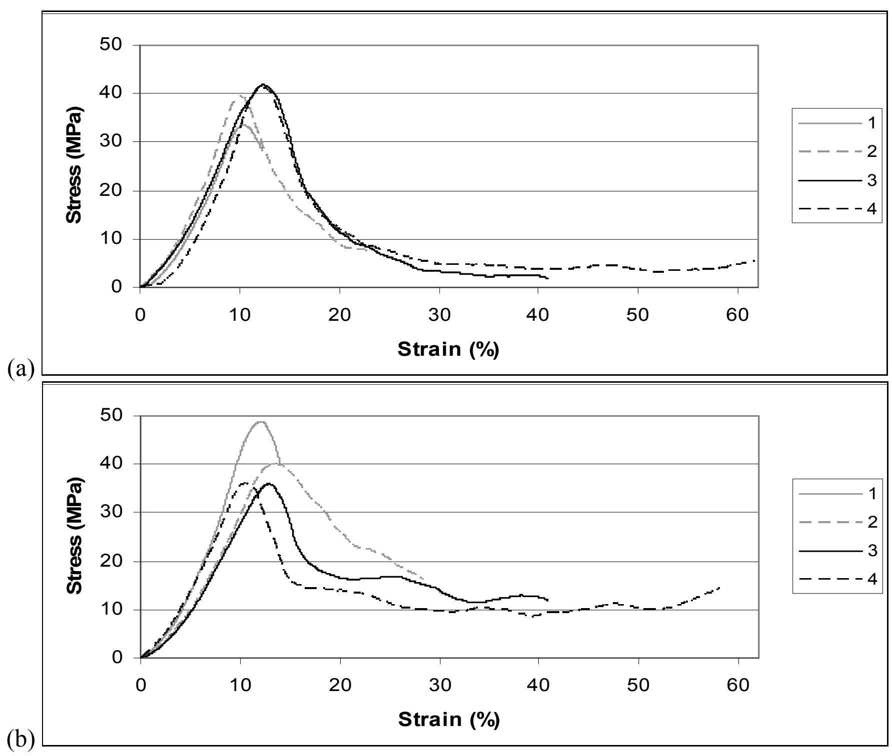

Figure 11. Stress-strain curves obtained from the four-stage interrupted compression tests of the composites with expanded clay particles: (a) fine granulometry; (b) coarse granulometry.

3.5 Analysis of the partially-compressed samples

One of the purposes of the interrupted compression test was to allow the analysis of the partially-compressed microstructures, and so to understand the mechanisms of deformation involved. Since there was not a significative influence of reinforcement particle sizes in the results, it will be presented only results according to the type of reinforcement (vermiculite or expanded clay).

In Figures 12 (a) and 13 (a), it is possible to observe that, in the first stage of deformation, the damage in the metallic walls is very similar for the two types of composite: the compression stress point corresponds to the rupture of some metallic walls. Fracture occurs in the eutectic component, located in the inter-dendritic region, and the cracks tended to propagate quickly. That fracture suggests a fragile behavior, and is considered to be the probable cause of the sudden decrease in stress that occurred after that point.

In Figures 12 (b) and 13 (b), it is possible to observe that, in the second stage of deformation, the damage in the metallic walls evolute differently according to the reinforcement material. In the composites with vermiculite, there are more consecutive cracks, and shear of walls, leading to fragmentation. That probably happens because of the geometry of the metallic walls, with many sharp reentrances originated from the open porosities of the reinforcement, resulting in more tension-concentrating points for the starting of cracks. In the composites with expanded clay, however, there are less cracks, but they occur mainly in a non-parallel way, with open angles, that suggest the rupture of reinforcement particles, thus supporting only some parts of metallic walls while letting other parts collapse.

In Figures 12 (c) and 13 (c) , it is possible to observe that, in the third or fourth stages of deformation, along with the increase of cracking and fragmentation, there are evidences of plastic deformation of the metallic material, mainly by compression, with the presence of deformed dendrites, which suggest that, after the collapse of metallic walls and reinforcement materials, they started to be compressed against each other, that is coherent with the densification stage. The results from the third and fourth stages are about the same, the only difference is that in stage 4 the failures observed become more frequent or more severe.

(a) (b) (c)

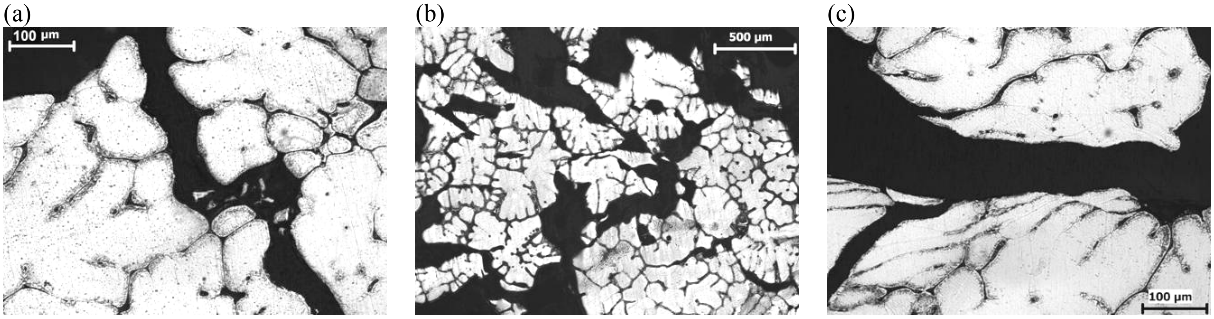

Figure 12. Sequence of optical microscopy images showing the damaged metallic structure of the composites with vermiculite particles, for different stages of compression: (a)1; (b)2; (c) 3 or 4. Samples etched with modified Keller's reagent.

(a) (b) (c)

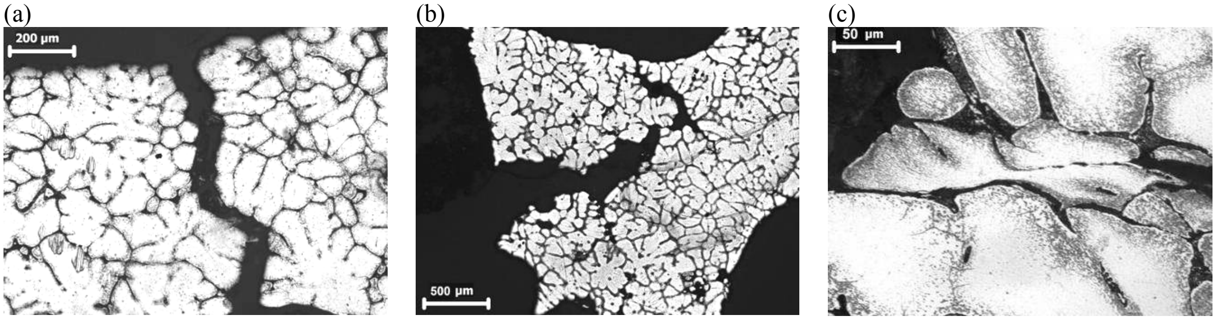

Figure 13. Sequence of optical microscopy images showing the damaged metallic structure of the composites with expanded clay particles, for different stages of compression: (a)1; (b)2; (c) 3 or 4. Samples etched with modified Keller's reagent.

For the expanded clay composites, there is another interesting fenomena observed: there are some cracks with continuity between the metallic matrix and the reinforcement (Fig. 14). That is an indicative of a very good coupling (adhesion) between the components, resulting in co-operation between matrix and reinforcement in bearing the mechanical efforts.

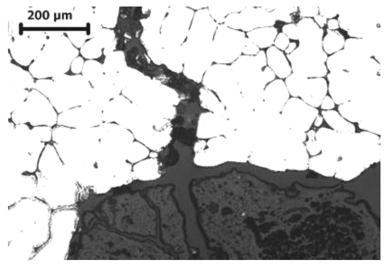

Figure 14. High bright optical microscopy image, showing the continuity of a failure crack between the metallic matrix and the reinforcement particle of expanded clay.

4. CONCLUSION

The composite materials, produced by semi-solid metallurgy process, showed good quality, indicating the suitability of the process. The use of low-density particles led to a low-density composite, with good distribution in the metallic matrix.

The mechanical behavior of the composites presents some similarities with the typical behavior of cellular metallic materials, showing a large plateau in the stress-strain curve, which suggests their capability of absorbing energy through their permanent deformation or crushing. The use of different reinforcement materials also reflected in different results in mechanical testing.

The high initial peak in their stress-strain curves, even though it is not expected for absorbing energy maintaining low force levels, can be a positive behavior if the application requires a good stiffness under normal loading and rupture (as circuit breakers) under excessive loading.

The analysis of the partially compressed samples helped to understand the deformation process, suggesting a correlation between the fracture of metallic walls and the sudden tension drop noticed in the stress-strain curves, and the influence of the mechanical interaction between the metallic matrix and the reinforcement particles in those results.

5. ACKNOWLEDGEMENTS

The authors would like to thank: CNPq, for the financial support, and Prof. Dr. Vitor Sordi from DEMa/UFSCar, for the access to the mechanical testing facilities.

6. REFERENCES

Motz, C., Pippan, R., Kriszt, B., 2002. “Mechanical Properties and Determination”. In: Degischer, H. P., Kriszt B. (Ed.). Handbook of Cellular Metals – Production, Processing, Applications. Wiley-VCH, Weinheim, Germany, pp. 183-202

Hatch, J. E. (Editor), 1993. “Aluminum: properties and physical metallurgy”. American Society for Metals, Ohio, USA, pp. 351-378. ISBN 0-87170-176-6

Jorge, A. F., Gatamorta, F, Arruda, A. C. F., Robert, M. H., 2010. “Produção de Materiais Compósitos Metálicos de Baixa Densidade”. ENMEC2010 - Encontro Nacional de Materiais e Estruturas Compósitas, FEUP, Porto, Portugal. (Proceedings in CD-ROM)

Kirkwood, D. H. *et alli*, 2010. “Semi-solid processing of Alloys”. Springer-Verlag, Berlin, Germany. ISBN 978-3-642-00705-7

Ashby, M. F. *et alli*, 2000. “Metal Foams: A Design Guide”, Butterworth-Heinemann, Woburn, MA, USA, 251p.

Silva, R.R., Robert, M.H., 2009. “Mechanical and structural characterization of open-cell Al alloys produced by thixoforming into removable space holders pre-forms”. 6th International conference on Porous Metals and Metallic Foams – MetFoam. Bratislava, Slovakia.

7. RESPONSIBILITY NOTICE

The authors are the only responsible for the printed material included in this paper.